COPY

OBTAINING CONSISTENT MODELS OF HELICOPTER FLIGHT-DATA MEASUREMENT ERRORS USING KINEMATIC-COMPATIBILITY AND STATE-RECONSTRUCTION METHODS

DTIC
ELECTE
JUN 0 4 1990
S D
D

Jay W. Fletcher
Aeroflightdynamics Directorate
U.S. Army Aviation Research and Technology Activity
Ames Research Center
Moffett Field, California

AD-A222 533

ABSTRACT

A new methodology has been developed for application of Kalman Filter/Smoothers to post-flight processing of helicopter flight test dynamic measurements. This processing includes checking for kinematic compatibility among the measurements, identification of a measurement error model, and reconstruction of both measured and unmeasured time histories. Emphasis is placed on identification of a parametric measurement error model which is valid for a *set* of flight test data. This is facilitated through a new method of concatenating several maneuver time histories. The methodology also includes a model structure determination step which ensures that a physically realistic parameterization has been achieved. Application of the methodology to a set of BO-105 flight test data is illustrated. The resulting minimally parameterized error model is shown to characterize the measurement errors of the entire data set with very little variation in the parameter values. Reconstructed time histories are shown to have increased bandwidths and signal-to-noise ratios.

NOMENCLATURE

a_x, a_y, a_z	= body axis translational accelerations (m/sec^2)
b	= bias error
B	= tracking bearing angle (rad)
$c.g.$	= center of gravity
E	= tracking elevation angle (rad)
f, g	= vector functions
g	= local gravitational acceleration (m/sec^2)
p, q, r	= body axis angular velocities (rad/sec)
R	= tracking range (rad)
t	= time
u, v, w	= body axis translational velocities (m/sec)
$\mathbf{u}$	= input vector
V	= total velocity (m/sec)
X, Y, Z	= Earth axis displacements w.r.t. tracking station (m)
$\mathbf{x}$	= state vector
$\mathbf{z}$	= observation vector
α	= angle of attack (rad)
β	= angle of sideslip (rad)
γ^2	= coherence function
δ	= pilot control deflection (%)
η	= random error
Θ	= error parameter
λ	= scale factor
ξ	= measured variable
τ	= time delay (sec)
ϕ, θ, ψ	= Euler angles (rad)

Presented at the 46th Annual Forum of the American Helicopter Society, Washington, DC, May 1990.

INTRODUCTION

High-quality flight test data is required for many applications in rotorcraft dynamics, controls, guidance, navigation, performance, and handling qualities analyses. However, obtaining accurate and complete flight test data is a difficult task. Measurements are always subject to sources of systematic and random error. In addition, some quantities may be difficult to measure directly. This is particularly true for helicopters because of the their high vibration levels, and is true of VTOL aircraft in general because of their large ranges of motion compared to conventional aircraft.

To achieve the necessary level of quality, errors in the flight test data must be detected and removed. This is possible because the kinematic quantities measured in flight are related to each other by well-known differential equations. The information in these equations can be used to determine the kinematic consistency (or compatibility) of the various measurements and to reconstruct others. This process is often called data consistency analysis and has been used as a precursor to such activities as system identification (1,2), simulation validation (3), and accident investigations (4).

DISTRIBUTION STATEMENT A
Approved for public release
Distribution Unlimited

90 05 29 131

Each of these methods has its own advantages and disadvantages. The objective of all of them, however, is to determine a model of flight data measurement errors. The validity of this model is of paramount importance because it will affect the validity of all subsequent analyses.

This paper presents a comprehensive, systematic methodology for conducting data consistency analyses using a previously developed state-estimation algorithm. The methodology was developed with the goal of achieving a robust technique for determining valid error models. In the process several new techniques were developed which may be of interest to others working in the field. The application of the methodology to a set of BO-105 flight test data is illustrated, and the validity and usefulness of the results are demonstrated.

The flight test data were produced by DLR, Institute for Flight Mechanics, Braunschweig, Germany, for use by AGARD Flight Mechanics Panel Working Group 18, "Rotorcraft System Identification," December 1987, and are used with permission.

BACKGROUND

Kinematic Equations

The set of kinematic equations for motions of the aircraft center of gravity with respect to a flat, non-rotating earth are presented in equations 1 through 15.

$$\dot{u} = rv - qw + a_x - g\sin\theta \tag{1}$$

$$\dot{v} = pw - ru + a_y + g\cos\theta\sin\phi \tag{2}$$

$$\dot{w} = qu - pv + a_z + g\cos\theta\cos\phi \tag{3}$$

$$\dot{\phi} = p + q\sin\phi\tan\theta + r\cos\phi\tan\theta \tag{4}$$

$$\dot{\theta} = q\cos\phi - r\sin\phi \tag{5}$$

$$\dot{\psi} = q\sin\phi\sec\theta + r\cos\phi\sec\theta \tag{6}$$

$$\dot{X} = u\cos\theta\cos\psi + v(\sin\phi\sin\theta\cos\psi - \cos\phi\sin\psi) + w(\cos\phi\sin\theta\cos\psi + \sin\phi\sin\psi) \tag{7}$$

$$\dot{Y} = u\cos\phi\sin\psi + v(\sin\phi\sin\theta\sin\psi + \cos\phi\cos\psi) + w(\cos\phi\sin\theta\sin\psi - \sin\phi\cos\psi) \tag{8}$$

$$\dot{Z} = -u\sin\theta + v\cos\theta\sin\phi + w\cos\theta\cos\phi \tag{9}$$

$$V = \sqrt{u^2 + v^2 + w^2} \tag{10}$$

$$\alpha = \arctan(w/u) \tag{11}$$

$$\beta = \arctan(v/u) \tag{12}$$

$$R = \sqrt{X^2 + Y^2 + Z^2} \tag{13}$$

$$E = \arcsin(-Z/R) \tag{14}$$

$$B = \arctan(Y/X) \tag{15}$$

For data consistency analyses, the equations are usually considered in the form of equations 16 and 17 with state, input, and observation vectors as defined in equations 18 through 20.

$$\dot{\boldsymbol{x}} = f(\boldsymbol{x}, \boldsymbol{u}) \tag{16}$$

$$\boldsymbol{z} = g(\boldsymbol{u}) \tag{17}$$

$$\boldsymbol{x}^T = [u, v, w, \phi, \theta, \psi, X, Y, Z] \tag{18}$$

$$\boldsymbol{u}^T = [a_x, a_y, a_z, p, q, r] \tag{19}$$

$$\boldsymbol{z}^T = [\phi, \theta, \psi, V, \alpha, \beta, R, E, B] \tag{20}$$

Measurement Errors

Measurement errors can be broadly classified as either deterministic, or random errors as shown in Figure 1. Bias and scale factor errors generally result from incorrect instrument calibrations. Typical sources of time skew errors are analog signal conditioning and multiplexing of digital data. Dropouts are usually present only in telemetered data or tracking data. Disturbance errors are caused when a sensor measures a motion not associated with the rigid-body rotation or translation of the aircraft center of gravity. A common example of disturbance errors is the effect of atmospheric turbulence on the measurement of the air-data variables. Quantization errors are caused by the analog-to-digital conversion process with finite digital word length. Other sources of random error include sensor and instrumentation noise and high frequency vibrations.

Measurement Error Models

A linear parametric model of measurement errors is generally adopted for data consistency analysis. Equations such as

$$\xi_e(t) = \lambda_\xi \cdot \xi_m(t - \tau_\xi) + b_\xi + \eta_\xi \tag{21}$$

relate the measured time histories, ξ_m, to the estimated time histories, ξ_e, through such parameters as bias errors, b_ξ, scale factors, λ_ξ, time delays, τ_ξ, and random errors, η_ξ. Some methods do not model the random error explicitly, and those that do generally assume it to be white gaussian. Time delay errors are seldom modeled, but some researchers have realized significant improvements in results by including them in the error model (9,10).

Data Consistency Analysis

Parameter values are determined by fitting the measured time histories to the estimated time histories subject to the constraints of equations 16 and 17. Differential equations for the deterministic error parameters are appended to to the state equations and provide additional constraints. These are usually trivial since the error parameters are usually assumed to be time-invariant.

Algorithms– Several algorithms have been used to identify parameter values and calculate estimated time histories. They differ mainly in the level of sophistication of their

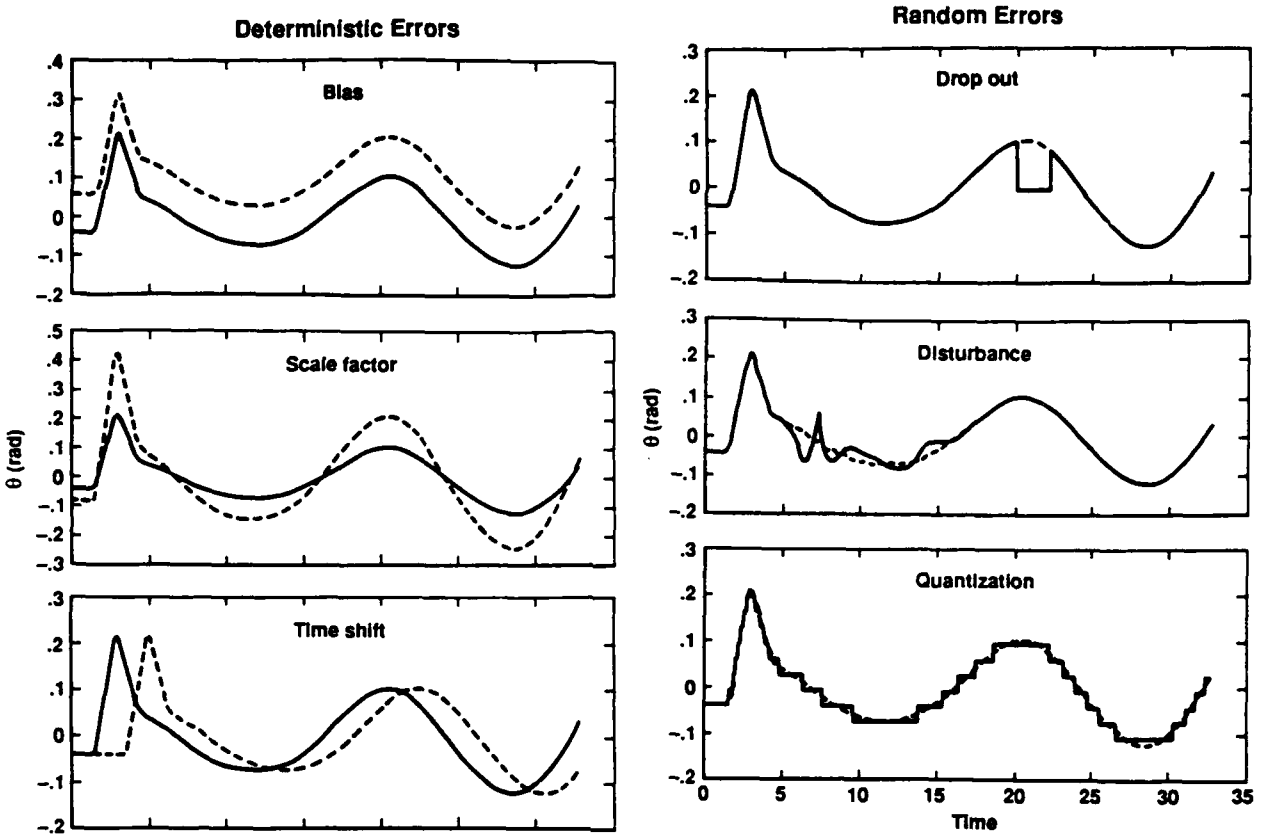

Fig. 1 Types of measurement errors.

constraints of equations 16 and 17. Differential equations for the deterministic error parameters are appended to to the state equations and provide additional constraints. These are usually trivial since the error parameters are usually assumed to be time-invariant.

Algorithms– Several algorithms have been used to identify parameter values and calculate estimated time histories. They differ mainly in the level of sophistication of their random error models and the type of cost function they employ. Some of the more common algorithms are discussed below.

Least Squares– Random errors are not modeled explicitly in this method. The state equations are integrated using measured state and input variables to calculate estimates of the state and output variables. This process continues, using estimated state values in further iterations, until parameter values are determined which minimize the least squares fit error between the measured and estimated outputs.

Extended Kalman Filter– Random errors in both the input variables (process noise) and output variables (measurement noise) can be modeled explicitly in this method. The presence of process noise means that the state variables must be treated as stochastic quantities. The Kalman filter steps through the data calculating estimates of the state and measurement variables based on models of the system dynamics and statistical properties of the process and measurement noise. Parameter values are determined through minimization of a cost function based on state and measurement variable fit errors weighted by the process and measurement error covariance matrices respectively.

Maximum Likelihood– The maximum likelihood identification technique is usually applied to the data consistency analysis problem as an output error (process noise neglected) formulation (8,9,10). This allows the state equations to be integrated directly. Random measurement errors are modeled explicitly by a covariance matrix. Parameter values are determined through minimization of the likelihood cost function which includes a weighted least squares measurement fit error term and an additional logarithmic term.

Model Structure Determination

The model structure refers to the set of non-zero parameters which are used to parameterize the measurement error. Determination of an appropriate model structure is an important part of any parameter identification problem. Improvements in the fit can almost always be achieved by adding non-zero parameters to the model. However, only parameters which truly represent a physical characteristic of the system should be included. An incorrect model structure

will cause the parameter estimates to be biased away from their true values.

Two factors which should be considered during model structure determination are parameter insensitivity and parameter correlation. If the solution (cost function) is relatively insensitive to variations in a particular parameter, then this parameter is said to have a high insensitivity. The parameter is then less likely to be an important part of the model structure, and removing it should be considered.

If variations in two or more parameters cause similar variations in the solution (cost function), then they are said to be correlated. The more two parameters are correlated, the less possible it is to determine unique values for each of them. This in turn makes it difficult to determine whether each of them is an important part of the model. This can be remedied by fixing one of them at an a priori value if enough information is available to determine a reasonable one.

METHODOLOGY

A comprehensive methodology has been developed for application of Kalman Filter/Smoothers to the identification of models for helicopter flight test data measurement errors. A flow chart of the information flow through this system is shown in Figure 2. The filter/smoother algorithm is applied in both the initial solution and final solution blocks. Some of the major features of the methodology are:

1. All of the flight test data for a given flight test is passed through a preprocessor whose function is to increase the signal-to-noise ratio of the data set.

2. A small subset of the preprocessed data is processed in an initial solution to obtain an initial error model structure for use as a start-up in the final solution. Knowledge of instrumentation characteristics is used at this step to determine appropriate values for the measurement error covariance matrix of the Kalman Filter.

3. All of the flight test data is then processed in the final solution step to obtain an error model valid for the entire set of data.

The final error-model parameters can be applied directly as corrections to the raw flight test data, or the filter/smoother can be used with the error parameters fixed to these values to reconstruct estimates of error-free time histories.

Each of the major sections of this process are explained in greater detail in the sections which follow.

SMACK

For the present study, the filter/smoother program SMACK (SMoothing for AirCraft Kinematics), developed by Ralph Bach at Ames Research Center, was employed as the parameter estimation/state reconstruction algorithm in the initial and final solution blocks. A block diagram of the

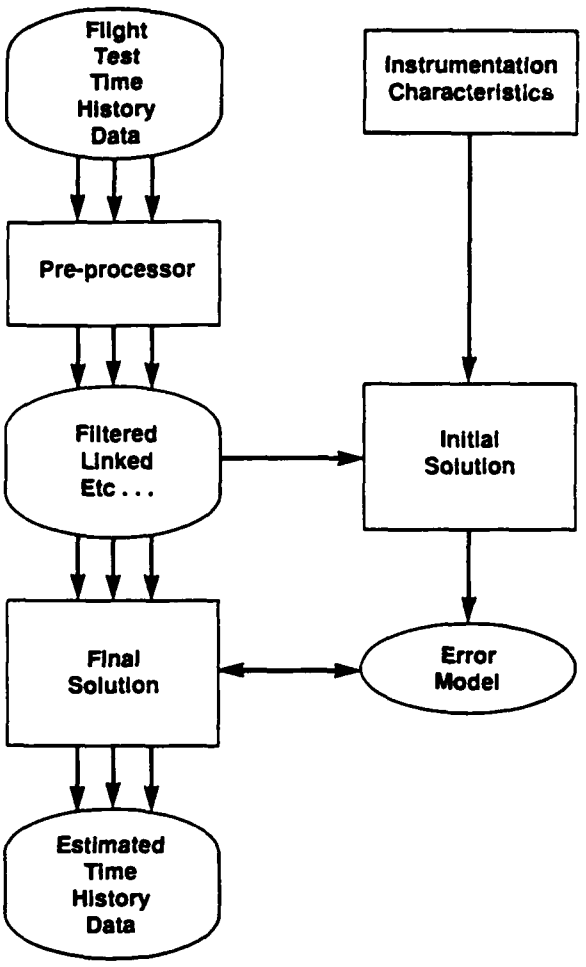

Fig. 2 Flow chart of developed methodology.

state and measurement models used by SMACK is shown in Figure 3. These models differ from the more commonly employed models of equations 18 through 20 because they have been formulated to keep the state model linear. All measured variables are also treated as observations and never as system inputs. Estimation of constant bias and scale factor errors in each of the measurements as well as time-varying winds is possible. Other algorithms could be substituted for SMACK without reducing many of the benefits of the overall methodology. However, SMACK has several properties and features which make it a favorable choice. These are discussed below.

Stochastic Optimal Estimator– The SMACK algorithm consists of a backward "information" filter and forward smoother. This formulation offers all of the advantages of the extended Kalman filter plus certain computational advantages which result in a more accurate and less computationally expensive solution (6). The use of a linear state model also improves the performance of the SMACK algorithm.

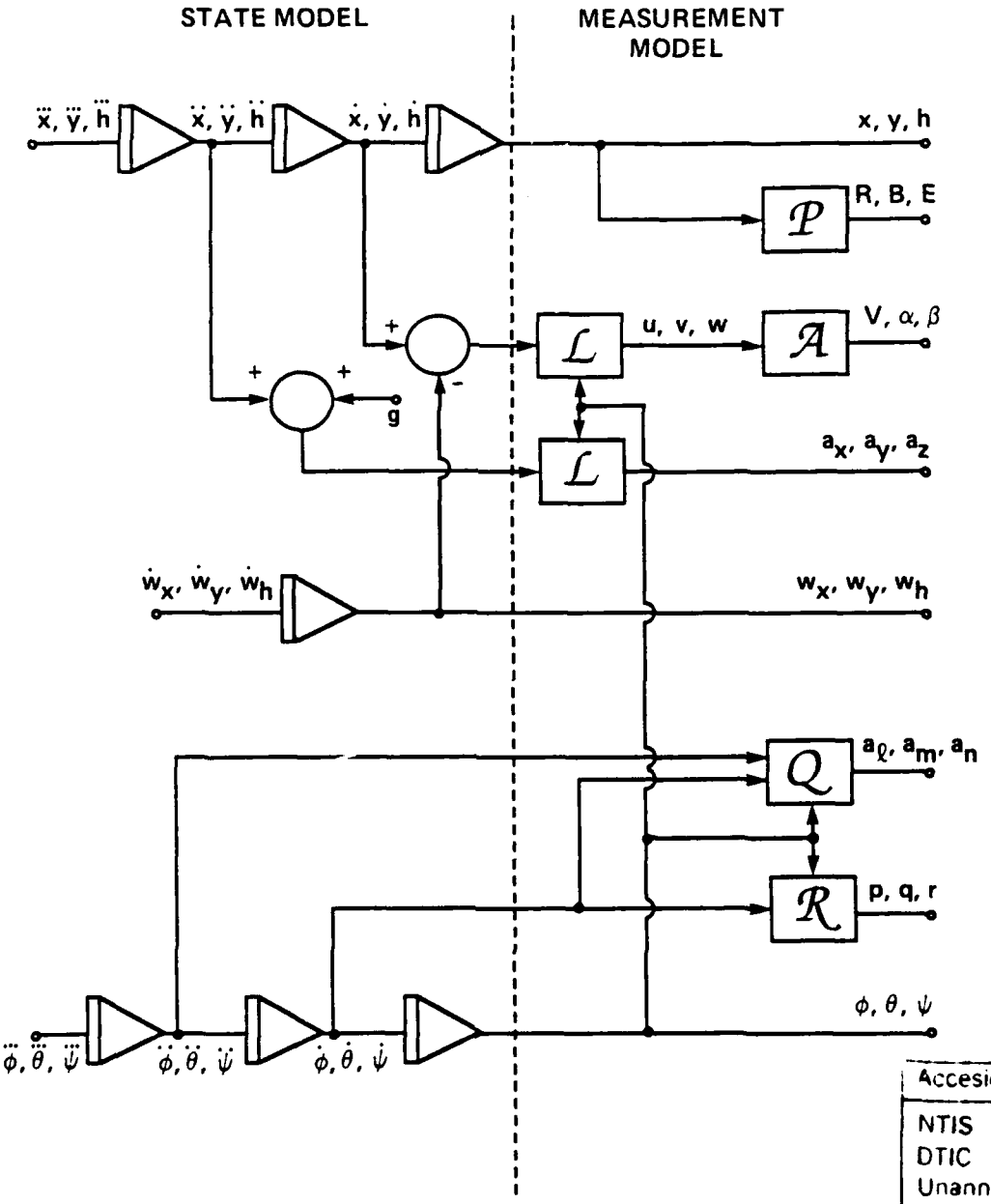

STATEMENT "A" per D. Kiefer
Army Aeroflightdynamics Directorate/FAZRT
AF-F, NASA Ames Research Center, Moffett Field, CA 94035
TELECON 5/31/90 VG

Fig. 3 State and measurement models used by SMACK.

DTIC COPY INSPECTED 6

Accesion For
NTIS CRA&I
DTIC TAB
Unannounced
Justification
By per call
Distribution /
Availability Codes
Dist | Avail and / or Special
A-1

Other Computational Features– SMACK calculates the means and standard errors of the final measurement residuals, which supplies a useful feedback to the user about the accuracy of initial estimates of the measurement error standard deviations. A provision is also supplied for the elimination of selected data points from the measurement update. This is very useful for elimination of disturbance-type errors from the measurements.

Convenience Features– A predefined measurement model is available, but new measurements are easily added. An internal simulated maneuver is available for debugging new input decks. Printed output provides many useful metrics of solution quality; and graphical output of measurement, estimate, and residual time histories is supplied.

Preprocessing

Studies have been conducted to investigate the variability of parameter values identified from different flight test maneuvers (1,7). This variability is often caused by poor excitation of some states for certain types of maneuvers. Klein (8) postulates that it may be possible to increase the accuracy of parameter estimates by designing an optimal maneuver. Indeed, this approach has been taken in a flight test program of the AV-8B Harrier aircraft conducted at the Ames Research Center (2). However, it is often the case that flight tests are conducted without this consideration in mind. The approach taken here is to create "optimal" maneuvers from sub-optimal flight test records in a preprocessing step.

Flight test time histories from several different types of maneuvers, usually one for each control axis, are concatenated to construct a composite maneuver with sufficient excitation of all kinematic quantities. Discontinuities at the junctions between events are avoided by inserting a buffer region of time between the records. These sections are flagged for elimination from the filter measurement update allowing SMACK to construct trajectories joining the two events. These "pseudo-dropouts" are of sufficient length to allow the estimated aircraft states to transition smoothly. When tracking data are available, coordinate transformations are made to the data to ensure a continuous flight path throughout the composite maneuver.

All of the flight test data are also carefully low-pass filtered to remove noise. This approach is taken because different types of sensors have different bandwidths. For instance, accelerometers will be much more sensitive to high-frequency vibrations than gyros will be. Thus, low-pass filtering removes another possible source of inconsistency among measurements.

Also, a visual inspection of the data is made and dropout and disturbance errors are flagged for elimination from the filter measurement update. This has the effect of increasing the signal-to-noise ratio of each affected measurement and removing a source of error which could otherwise bias estimates of the error model parameters.

Use of this preprocessing procedure has resulted in less variation in identified parameter values and improved time history estimates.

Initial Solution

The objective of the initial solution step is to determine an initial error model structure and refine estimates of the measurement error covariance values. This analysis is performed by iteratively processing one representative composite maneuver through SMACK. The results are used as a start-up for processing of all of the cases in the final solution.

The initial values of the measurement error covariances are determined from the digital resolution of the instrumentation system. This information is usually available from calibration data for each measured channel as the number of engineering units per "count."

For example, a typical 12-bit system would provide a maximum of $2^{12} = 4096$ counts per channel. If an accelerometer was calibrated to read –1.00g at 1600 counts and +1.50g at 2800 counts, the digital resolution of that channel would be 2.50g/1200 = 0.00208g.

These values are input to SMACK as the standard deviations of the random error component of the measurement errors. This is compatible with the requirements of the filter/smoother since quantization error can be modeled as white noise (12, pages 190-195) . The assumption that all of the random error may be attributed to quantization effects is sufficiently accurate for starting up the initial solution process. In fact, it is likely that low-pass filtering has removed most other sources.

The representative case is then processed iteratively through SMACK. After each iteration, the error model structure and error covariance values may be modified based on evaluation of the three following criteria.

Measurement Residuals– In his forthcoming NASA Reference Publication "State Estimation Applications in Aircraft Flight-Data Analysis (A User's Guide for SMACK)," Bach states that one of the criteria for a "good" SMACK solution is that all of the residuals should be white, zero mean, and have standard deviations close to the measurement error standard deviation values provided by the user. This concept is similar to the Innovations Property of linear-optimal filters (13, page 400) .

At each iteration of the initial solution the residuals are examined for whiteness, offset, and magnitude. Non-white or non-zero mean residuals may be indicative of error-parameters which are missing from the model. A missing scale factor will cause the corresponding residual signal to have a shape similar to the measured signal. A missing bias parameter will cause the residual to have a non-zero mean value.

The standard errors of the residuals are compared to the user-supplied estimates of the measurement error standard deviations. If a residual is sufficiently white, then its standard error will be a good measure of the true measurement error standard deviation. If not, an estimate of the standard error of the random portion of the residual signal may have to be made. The user may then update his estimates accordingly.

Parameter Insensitivity– The insensitivity of the model to variations in its parameters is determined through examination of the parameter Cramer-Rao lower bounds generated by SMACK. It is well known that the Cramer-Rao bounds overestimate the accuracy of the identified parameter, but they are useful for comparisons of relative accuracy between parameters, and variations from case to case (10). When the ratio of the Cramer-Rao bound to the parameter value is relatively large (usually by a factor of ten) for a particular parameter, it is eliminated from the model structure. It has been the author's experience that there is little effect on the whiteness of the residuals from elimination of insensitive parameters.

Of course, physical understanding of a particular problem should always be used to pare down a model structure from the outset. For example, if one is conducting an analysis of the three rotational degrees-of-freedom only, the solution will be very insensitive to bias errors in ϕ and θ. For a six-degree-of-freedom analysis without tracking data the solution will be completely insensitive to a bias error in ψ. This is readily verified through inspection of the kinematic equations.

Parameter Correlation– No numerical indicator of parameter correlation is presently calculated in SMACK. Correlation of parameters is currently avoided by consideration of the the structure of the kinematic equations and use of non-kinematic information. For example, bias errors in a_x and θ will be highly correlated. The kinematic equations reveal the correlation, but more information is needed to determine which measurement is really biased. If the flight test data includes segments of trimmed flight, then pilot comments or simulation results may be used to determine the validity of the measured trim attitude.

Convergence– The above criteria are examined at each iteration until an appropriate model structure and measurement error covariance values are obtained. Convergence problems have not been encountered.

Final Solution

The direction in which the analysis proceeds from this point depends on the characteristics of the database. If the flight tests were conducted over a long period of time, then it is likely that the instrumentation characteristics will vary significantly throughout the database. In this case we can expect the error model structure and parameter values to vary, and the procedure of the initial solution will have to be applied enough times to capture this variation. However, if the flight tests are conducted within a short enough period of time, the assumption of a stationary error model can be made. In this case the procedure of the final solution is employed to determine a model structure and parameter values valid for the entire data base.

In the final solution step, SMACK is applied iteratively to all of the composite maneuver cases. At each iteration, the error-model structure is held constant across all the maneuvers. The model structure from the initial solution is used as a start-up in this process.

After each iteration, the sample mean values and standard deviations of the parameters are calculated. The parameter with the largest variation above a certain threshold is dropped from the model. This process continues until all of the parameters have sufficiently small variations.

It has been the author's experience that an appropriate threshold value of parameter variation usually appears during the analysis. The parameters are usually grouped into sets with low-variance and high-variance. Sequential elimination of the high-variance parameters tends to reduce the variations in the low-variance parameters, accentuating this division. Determination of an appropriate threshold value is therefore a simple matter.

When a final solution is determined, the model structure and parameter values are enforced in SMACK to reconstruct time histories of measured and unmeasured variables for each of the unlinked flight test events.

RESULTS

The proposed methodology has been applied to a set of flight test data produced by the DLR, Institute for Flight Mechanics in Braunschweig, Germany, for use in time- and frequency-domain parameter identification (1). These tests were flown in the DLR ATTHeS BO-105 helicopter (see Figure 4). The data include doublet, multi-step "3211", and frequency-sweep maneuvers in each of the four control axes. The doublets were repeated twice in each direction; the 3211's were repeated three times in each direction; and the frequency-sweeps were repeated three times for a total of 52 flight test events. The nominal flight condition was horizontal flight at 80 knots and a density altitude of 3000 feet, and the entire flight test was conducted in less than two weeks. The measurements used in consistency checks and state reconstruction included: the Euler angles ϕ and θ; body angular rates p, q, and r; c.g. specific forces a_x, a_y, and a_z; and c.g. translational velocities u, v, and w. The translational velocities had previously been derived from measurements taken with a HADS air data system which uses a swiveling pitot static mechanism located below the main rotor.

The 52 flight test events were preprocessed into 13 composite maneuvers, each consisting of a longitudinal cyclic maneuver, a lateral cyclic maneuver, a collective maneuver,

Fig. 4 DLR ATTHes BO-105 helicopter.

and a pedals maneuver. Disturbance errors in the velocity signals were discovered in many of maneuvers. It is believed that these were caused by interaction of the HADS air data sensor with the rotor wake. They were flagged for elimination from the filter measurement update.

Parameter values for the final model structure are tabulated for the 13 composite maneuvers in Table 1. The SMACK calculated Cramer-Rao lower-bounds are also tabulated. The standard deviations of all of the parameters are less than 11% of their respective mean values. Such small variations in the parameter estimates validate the assumption of a stationary error model and provide a high degree of confidence in the model structure and parameter mean values themselves. It is also notable that the Cramer-Rao bounds underestimate the sample variations by as much as two orders of magnitude.

The usefulness of the composite maneuver approach can be seen by comparing the results in Table 1 with those in Table 2. The parameter values in Table 2 were obtained using the same model structure, but the individual flight test maneuvers were used in the identification instead of the composite maneuvers. It is evident that the standard deviations of the parameters increase and their mean values change significantly when this approach is taken.

The effect of excitation of a particular variable on the identification of error parameters associated with it can be seen in Table 3. Here the identified values for the scale factor on lateral velocity are tabulated by the control axis of the maneuver. It is clear that variations in the identified value of λ_v are smaller for the pedal and lateral cyclic maneuvers which contain much larger lateral velocity responses than the other maneuvers.

Comparison of filtered flight test data and reconstructed time histories for a typical composite maneuver is illustrated in Figure 5. The reconstructed data have been decorrected by the identified error parameters for plotting purposes. Also, the "pseudo-dropouts" between events have been removed to improve the plot scales. Only lateral variables are plotted to save space, but the results are representative of the the fits in other axes.

The consistency is generally very good. The lack of remaining deterministic errors indicates that the error model

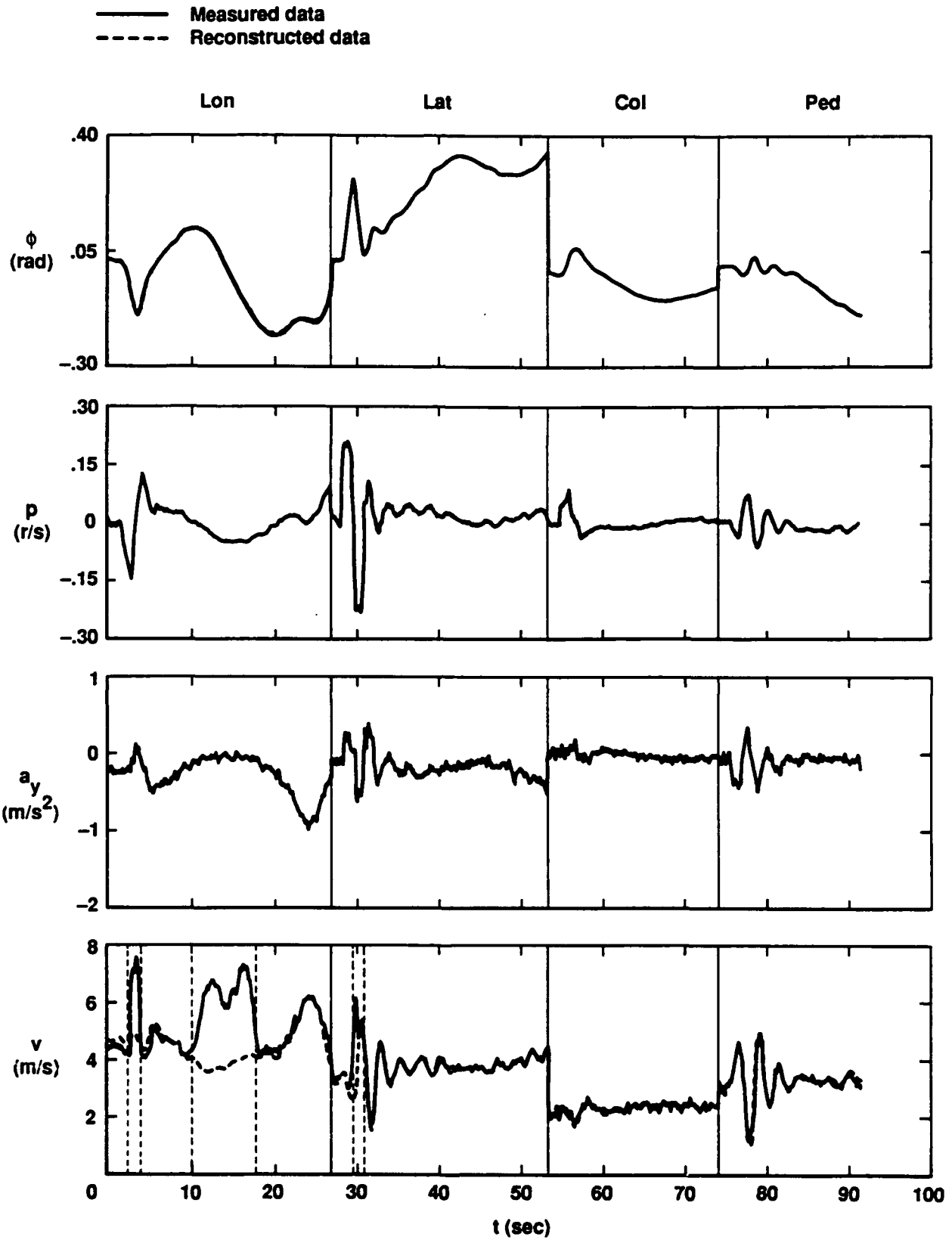

Fig. 5 Comparison of BO-105 measured and reconstructed time histories.

Table 1 Error model parameters identified for composite maneuvers

Case	b_p (d/s)	b_q (d/s)	λ_u	λ_v	λ_w
1	0.0805±0.0003	0.0862±0.0003	0.9600±0.0002	0.6900±0.0008	0.8277±0.0009
2	0.0743±0.0003	0.0894±0.0003	0.9746±0.0003	0.7286±0.0011	0.8651±0.0009
3	0.0807±0.0003	0.0851±0.0003	0.9446±0.0002	0.7495±0.0011	0.8137±0.0010
4	0.0930±0.0003	0.0836±0.0003	0.9940±0.0003	0.7321±0.0011	0.8840±0.0012
5	0.0949±0.0003	0.1050±0.0003	0.9681±0.0003	0.6422±0.0007	0.8748±0.0008
6	0.0937±0.0003	0.0914±0.0003	0.9425±0.0002	0.6748±0.0007	0.8573±0.0007
7	0.0848±0.0002	0.1094±0.0002	0.9541±0.0002	0.6408±0.0008	0.8859±0.0006
8	0.1089±0.0003	0.1054±0.0003	0.9572±0.0002	0.7679±0.0009	0.8995±0.0007
9	0.0793±0.0002	0.1022±0.0002	0.9082±0.0002	0.6479±0.0008	0.8120±0.0007
10	0.0857±0.0002	0.1081±0.0002	0.9344±0.0001	0.7105±0.0008	0.9083±0.0006
11	0.0779±0.0001	0.0918±0.0001	0.9438±0.0002	0.7065±0.0007	0.9107±0.0007
12	0.0826±0.0001	0.0930±0.0001	0.9968±0.0002	0.8171±0.0010	0.9349±0.0009
13	0.0850±0.0001	0.0926±0.0001	1.0010±0.0003	0.7280±0.0014	0.8763±0.0010
$\Theta \pm \sigma_\Theta$	0.0863±0.0093	0.0956±0.0091	0.9556±0.0272	0.7043±0.0524	0.8750±0.0378

adequately characterizes those present in the flight data. Disturbance errors are evident in the lateral velocity measurement. Vertical dotted lines indicate the regions of the signal which have been eliminated from the measurement update. The missing velocity segments have been satisfactorily reconstructed.

Improvements in the velocity signals are also clearly seen in the frequency domain. The frequency responses for lateral velocity due to pedal inputs identified using measured and reconstructed lateral velocity signals are compared in Figure 6. Bode magnitude and phase and the coherence function γ^2 are plotted. The coherence function indicates the fraction of the output which can be accounted for by linear relation with the input. It may be reduced from a maximum value of 1 by nonlinearities, input and output noise, and lack of excitation and/or response. The most striking feature of Figure 6 is that the coherence function for the response identified from the reconstructed data is larger over a much wider frequency range. This is the result of two factors. The first is that the signal-to-noise ratio of the lateral velocity signal has been increased through the elimination of random and disturbance errors. The second is that the bandwidth of the lateral velocity signal has been increased by the complementary filter action of the Kalman Filter. This results from the use of many measurements with different response characteristic in the calculation of the reconstructed time histories.

It is also interesting to note that, for the range of frequencies where both frequency responses have high coherence values, their response characteristics are very similar. The only major difference is a magnitude shift of approximately 3dB which agrees with the $\lambda_v = 0.71$ identified in the time domain. This also indicates that the state-estimation process has not corrupted the dynamic relationship between the control and response variables.

The results presented here have been used in time- and frequency-domain identification and verification of BO-105 dynamic models. Improvements in the identifications were obtained for use of the identified parameters in the time-domain method and use of reconstructed data in the frequency-domain method (1).

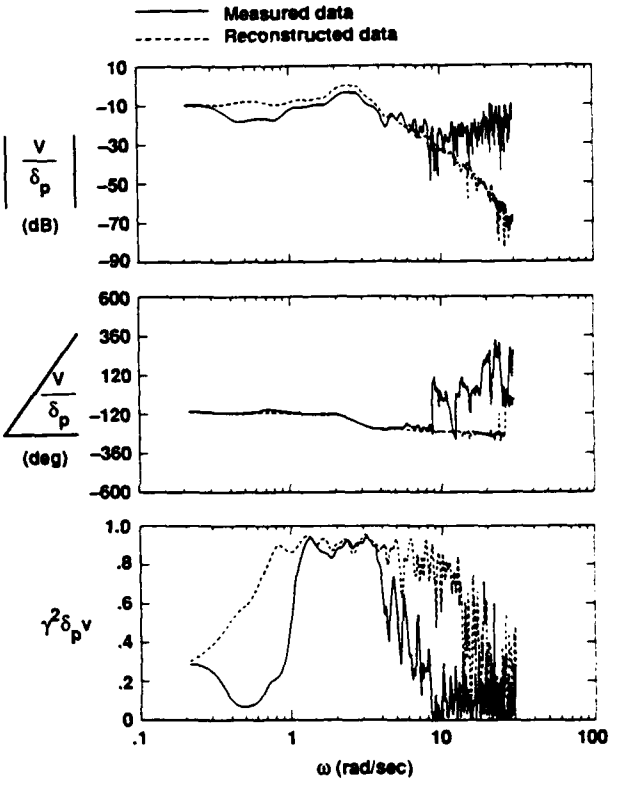

Fig. 6 Comparison of frequency responses identified from flight test and reconstructed data.

CONCLUDING REMARKS

A comprehensive and systematic methodology for identifying models of helicopter flight data measurement errors has been developed. This methodology makes use of the favorable properties and features of the optimal filter/smoother program SMACK. A preprocessing step is used to construct composite maneuvers with increased kinematic information content and to increase the signal-to-noise ratios of individual measurements. Appropriate measurement error covariance values are determined in an initial solution step, and a

Table 2 Error model parameters identified for flight test maneuvers

Case	b_p (d/s)	b_q (d/s)	λ_u	λ_v	λ_w
1	0.0933	0.0930	0.9472	0.6684	0.8181
2	0.0835	0.1016	1.0010	0.9543	0.8986
3	0.0895	0.0814	0.9465	0.6760	0.7989
4	0.0825	0.0697	0.9880	1.0080	0.9206
5	0.0353	0.0691	1.0390	0.6840	0.8834
6	0.0414	0.0959	1.1030	0.8070	1.0140
7	0.0920	0.0783	0.9392	0.8276	0.8185
8	0.1054	0.1025	1.0100	0.7776	0.9546
9	0.0803	0.0817	0.9969	1.0610	0.8723
10	0.0719	0.0771	0.8741	0.3801	0.6621
11	0.0607	0.0734	0.9432	0.7079	0.8363
12	0.1087	0.0873	0.9648	0.5633	0.7920
13	0.0890	0.0853	0.9511	0.6546	0.8519
14	0.1278	0.0753	1.1560	0.7695	0.9907
15	0.0625	0.1246	1.0140	0.7400	0.8646
16	0.0562	0.0832	1.0610	0.7548	0.8791
17	0.1717	0.2329	1.0230	1.6270	0.8639
18	0.0955	0.0798	0.9454	0.6182	0.8548
19	0.1454	0.0792	0.9460	0.9846	0.8053
20	0.1115	0.1292	0.8733	0.3846	0.7930
21	0.0692	0.0875	0.8815	0.9083	0.7627
22	0.0860	0.1099	0.8918	0.5254	0.8839
23	0.0839	0.0825	0.9895	0.5860	0.8744
24	0.0922	0.1016	0.9693	0.6867	0.9216
25	0.0852	0.1214	0.9390	0.4398	0.8797
26	0.1142	0.1572	0.9745	0.7874	0.8078
27	0.0753	0.1118	0.9119	0.9411	0.9201
28	0.0791	0.1448	0.9119	0.8493	0.9372
29	0.0896	0.1132	0.9660	0.8372	0.9252
30	0.0789	0.0779	0.9132	0.9084	0.8790
31	0.0752	0.0828	0.9005	0.8295	0.6680
32	0.0821	0.0757	0.9601	0.7037	0.9101
33	0.0834	0.1083	0.9151	0.5536	0.8495
34	0.0838	0.0816	0.9564	0.6686	0.7682
35	0.0897	0.0760	0.9436	0.6310	0.8044
36	0.1026	0.1092	0.9276	0.6411	0.8165
37	0.0676	0.1209	1.0010	0.6540	0.8345
38	0.1123	0.0939	0.9727	0.8419	1.0580
39	0.0872	0.1079	0.9306	0.5956	0.7921
40	0.0894	0.0908	0.9616	0.6751	0.9224
41	0.0569	0.0930	0.8370	0.5546	0.7126
42	0.0756	0.0928	0.9479	0.7819	0.8639
43	0.0750	0.0933	0.8803	0.6354	0.7844
44	0.0745	0.0933	0.7987	0.4792	0.7732
45	0.0692	0.0925	0.8289	0.5846	0.8208
46	0.0742	0.0918	0.9143	0.6473	0.8498
47	0.0961	0.0909	0.9895	0.7911	1.1930
48	0.1069	0.0950	1.0360	1.0310	1.1300
49	0.0843	0.0918	0.8794	0.6546	0.7299
50	0.0799	0.0904	0.8518	0.5467	0.6609
51	0.0728	0.0913	0.9640	0.7113	0.7628
52	0.1044	0.0940	1.0880	0.7037	0.8520
$\bar{\Theta}$	0.0849	0.0955	0.9488	0.6764	0.8432
σ_Θ	0.0230	0.0265	0.0687	0.2095	0.1031

Table 3 Variation in λ_v identification with level of lateral velocity excitation for different control axis inputs

Case	δ_{ped}	δ_{lat}	δ_{col}	δ_{lon}
1	0.6546	0.6840	1.0610	0.6684
2	0.7695	0.8070	0.3801	0.9543
3	0.7400	0.8276	0.7079	0.6760
4	0.7548	0.7776	0.5633	1.0080
5	0.6310	0.5860	0.8372	1.6270
6	0.6411	0.6867	0.9084	0.6182
7	0.6540	0.4398	0.8295	0.9846
8	0.8419	0.7874	0.7037	0.3846
9	0.5956	0.9411	0.5536	0.9083
10	0.6751	0.8493	0.6686	0.5254
11	0.5467	0.4792	0.7911	0.5546
12	0.7113	0.5846	1.0310	0.7819
13	0.7037	0.6473	0.6546	0.6354
$\bar{\Theta}$	0.6728	0.6581	0.7098	0.6732
σ_Θ	0.0801	0.1556	0.1963	0.3402

measurement error model valid for a set of flight test data is identified in a final solution step.

This methodology had been applied to the identification of a physically realistic measurement error model for a set of BO-105 flight test data. The identified model is described by a small number of parameters which each vary less than 11% over the entire data base. The use of composite maneuvers in the identification was shown to decrease variations in the parameter values.

Reconstructed time histories were shown to be free of many deterministic and random errors. This included the elimination of rotor wake interference effects from the velocity measurements. Frequency response analysis demonstrated that these signals have increased bandwidths and signal-to-noise ratios.

Use of the results of the BO-105 data consistency analysis in identification of BO-105 dynamic models has produced improvements in the identification results.

REFERENCES

[1] Kaletka, J., Von Grünhagen, W., Tischler, M. B., and Fletcher, J. W., "Time and Frequency-Domain Identification and Verification of B0-105 Dynamic Models," Proceedings of 15th European Rotorcraft Forum, Amsterdam, Netherlands, Sept. 1989.

[2] McNally, B. D. and Bach, R. E., Jr., "Flight Testing a V/STOL Aircraft to Identify a Full-Envelope Aerodynamic Model," NASA TM-100996, 1988, also AIAA Paper 88-2134-CP.

[3] Ballin, M. G., "Validation of the Dynamic Response of a Blade-Element UH-60 Simulation Model," Proceedings of the 46th Annual AHS Forum, Washington, DC, May 1990.

[4] Bach, R. E., Jr. and Wingrove, R. C., "Analysis of Windshear from Airline Flight Data," Journal of Aircraft, Vol. 26, No. 2, Feb. 1989, pp. 103-109.

[5] Gilbert, N. E. and Williams, M. J., "Preliminary Kinematic Consistency Checking of Helicopter Flight Data," Aeronautical Research Laboratory, Melbourne, Australia, ARL-AERO-NOTE-414 (AR-002-935), 1982.

[6] Bach, R. E., Jr. and Wingrove, R. C. "Applications of State Estimation in Aircraft Flight-Data Analysis," Journal of Aircraft, Vol.22, No.7, July 1985, pp. 547-554.

[7] Klein, V. and Schiess, J. R., "Compatibility Check of Measured Aircraft Responses Using Kinematic Equations and Extended Kalman Filter," NASA TN-D-8514, 1977.

[8] Klein, V. and Morgan, D. R., "Estimation of Bias Errors in Measured Airplane Responses Using Maximum Likelihood Method," NASA TM-89059, January, 1987.

[9] Feik, R. A., "On the Application of Compatibility Checking Techniques to Dynamic Flight Test Data," ARL-AERO-REPORT-161 (AR-003-931), 1985.

[10] Feik, R. A., "Data Compatibility Checking of Helicopter Flight Measurements," ARL-FLIGHT-MECH-TM-416 (AR-005-650), August 1989.

[11] Parameswaran, U. C. and Niranjan, J. R. R., "Estimation of States of Aircrafts by Kalman Filtering Algorithms," National Aeronautical Laboratory, Bangalore, India, PD SE 8810, July 1988.

[12] Franklin, G. F. and Powell, J. D., Digital Control of Dynamic Systems, Addison-Wesley, Reading, Massachusetts, 1980.

[13] Stengel, R. F., Stochastic Optimal Control, John Wiley & Sons, Inc., New York, 1986.